Experimental and Kinetic Study on Ignition Delay Times of Di-n-butyl Ether at High Temperatures

ARTICLE *in* ENERGY & FUELS · AUGUST 2014

Impact Factor: 2.79 · DOI: 10.1021/ef500873e

5 AUTHORS, INCLUDING:

Li Guan
Xi'an Jiaotong University
5 PUBLICATIONS **4** CITATIONS
SEE PROFILE

Chenglong Tang
Xi'an Jiaotong University
72 PUBLICATIONS **733** CITATIONS
SEE PROFILE

Ke Yang
Xi'an Jiaotong University
5 PUBLICATIONS **4** CITATIONS
SEE PROFILE

Zuohua Huang
Xi'an Jiaotong University
419 PUBLICATIONS **5,178** CITATIONS
SEE PROFILE

energy&fuels

Article

pubs.acs.org/EF

Experimental and Kinetic Study on Ignition Delay Times of Di-*n*-butyl Ether at High Temperatures

Li Guan, Chenglong Tang,* Ke Yang, Jun Mo, and Zuohua Huang*

State Key Laboratory of Multiphase Flows in Power Engineering, Xi'an Jiaotong University, Xi'an, Shaanxi 710049, People's Republic of China

Supporting Information

ABSTRACT: Ignition delay times of di-*n*-butyl ether (DBE)/oxygen mixtures diluted with argon were measured behind reflected shock waves for the pressures between 1.2 and 4 bar, the temperatures between 1100 and 1570 K, and the equivalence ratios of 0.5, 1.0, and 1.5. A recently developed DBE model was employed to simulate the autoignition process of the homogeneous mixture. Comparisons between the measured and calculated ignition delay times indicate that the model yields fairly good agreement under all test conditions. Results show that the ignition delay time increases with the decrease of the pressure and the increase of the dilution ratio. The ignition delay time demonstrates a strong negative dependence upon the equivalence ratio at high temperatures, and the difference among the ignition delay times tends to decrease when the temperature is decreased. Sensitivity analysis reveals the importance of H-abstraction reactions and decomposition of α fuel radicals in the ignition process of DBE. Reaction pathway analysis confirms that the consumption of DBE is dominated by the H-abstraction reactions at lower temperatures, and when the temperature is increased, the unimolecular decomposition reactions become more important. Comparisons of ignition delay times as well as fuel consumption and radical growth history of DBE to dimethyl ether (DME) and diethyl ether (DEE) for given equivalence ratios indicate that DBE has the strongest overall reactivity, although the reactant concentration of DBE is the lowest.

1. INTRODUCTION

To decrease the consumption of fossil fuels and meet the increasingly stringent vehicle emission regulations, research to look for clean alternative fuels has attracted more attention recently. During the past decade, ethers, such as dimethyl ether (DME) and diethyl ether (DEE), have received significant attention because of their great potential for pollutant reduction and easy production through the dehydration of alcohols.[1−4] In comparison to the short-chain ethers, such as DME and DEE, di-*n*-butyl ether (DBE) has even better attributes: It can be produced from lignocellulosic biomass,[5] which does not threaten the food supply and biodiversity. It also has higher volumetric energy density, higher octane number, and higher boiling temperature, which favor its substitution for diesel fuels.

Extensive work on spray and combustion characteristics of DME and DEE[6−10] has been conducted. Several detailed kinetic models of DME[11−15] and DEE[16] have also been reported previously. However, investigations of DBE, neither practical nor in terms of fundamental combustion, have been scarce. Beeckmann et al.[17] studied the spray characteristics of various blends of the oxygenated compound di-*n*-butyl ether (DBE) with standard EN590 diesel fuel in a spray chamber under ambient conditions of 50 bar and 800 K. Their results showed that the spray structure of the DBE alone and its blends with diesel fuel presented a larger spray angle and shorter penetration length compared to pure diesel fuel; thus, it was potentially capable of improving atomization and engine performance. Nabi et al.[18] studied the ignition delay, brake-specific energy consumption, and exhaust gas emissions in a diesel engine with a wide range of DBE−diesel fuel blends. Their work showed that with the increase of the DBE blending ratio, significant reductions in smoke, CO, NO_x, and total hydrocarbon (THC) were simultaneously achieved; meanwhile, engine noise was reduced because of better ignitibility of DBE. Fundamentally, Harry et al.[19] studied the rate constants for the gas-phase reactions of OH radicals with DBE, at a temperature of 296 ± 2 K and atmospheric pressure. More recently, Cai et al.[20] measured the low-temperature ignition delay times at atmospheric pressure using a laminar flow reactor (LFR). Additionally, the laminar flame speeds of DBE/air mixtures in the stagnation flame configuration were also collected. A chemical kinetic model covering low- and high-temperature kinetics was developed and yielded fairly good agreement with their experimental results.

Our first objective of this study is to provide the ignition delay times of DBE/O_2/Ar mixtures over a wide range of equivalence ratios, temperatures, and pressures, using our well-developed shock-tube facility. Additionally, these measured ignition delay times will be used as the data for validation of a recently developed kinetic mechanism.[20] Furthermore, the oxidation kinetics of DBE will be examined in detail, to reveal the most sensitive reactions that dominate the ignition delay time predictions, and sensitivity analysis and reaction pathway analysis were performed to reveal potential reasons for different simulation results using the above models. Finally, comparative research of the ignition delay times of DME, DEE, and DBE will be conducted.

Received: April 20, 2014
Revised: July 2, 2014
Published: July 3, 2014

   dx.doi.org/10.1021/ef500873e | *Energy Fuels* 2014, 28, 5489−5496

2. EXPERIMENTAL SECTION

Measurements were carried out in a shock tube with a diameter of 11.5 cm, which is divided into a 4 m long driver section and a 5.3 m long driven section, separated by double polyethylene terephthalate (PET) diaphragms. Details of the facility was previously described.[21,25] Diaphragms with different thicknesses were chosen at different pressures. Before each run, the tube was evacuated to the pressure below 10^{-6} bar to ensure the purity of the system. Fuel mixtures of DBE (purity > 99.95%), oxygen (purity > 99.999%), and argon (purity > 99.999%) were prepared in a 128 L stainless mixing tank and allowed to mix for at least 12 h. A high-accuracy pressure transmitter (Rosemount 3051) was used to record the partial pressure of each component. The partial pressure of DBE in all mixtures was assured to be less than 50% of its saturated vapor pressure at the tank temperature to avoid fuel condensation. Table 1 lists the composition of seven mixtures of DBE, DME, and DEE in this study, in which ϕ is the equivalence ratio and D is the dilution ratio (X_{Ar}/X_{O_2}).

Table 1. Gas Composition of Fuel/O_2/Ar Mixtures in This Study

fuel	mixture	ϕ	D	fuel (%)	O_2 (%)	Ar (%)
	1	1	21	0.377	4.528	95.094
	2	1.5	15.5	0.752	6.015	93.233
DBE	3	1	15.5	0.503	6.030	93.467
	4	0.5	15.5	0.252	6.045	93.703
	5	1	9.9	0.759	9.105	90.137
DEE	6	1	15.5	1	6	93
DME	7	1	15.5	1.98	5.94	92.079

Figure 1 shows the definition of the ignition delay time. It is defined as the time interval between the arrival of the incident shock wave

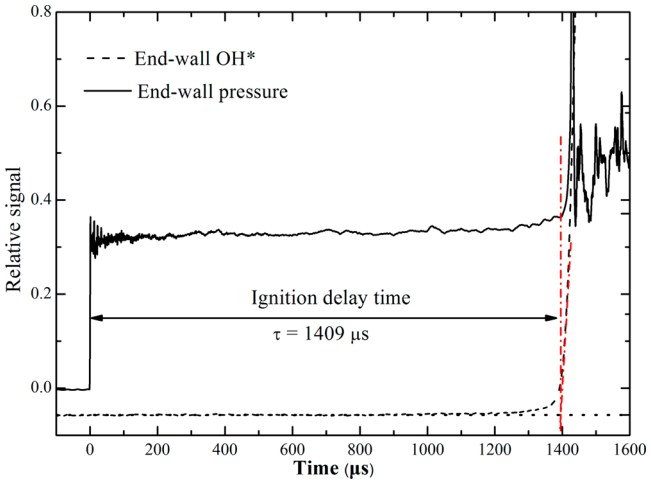

Figure 1. Determination of the ignition delay time of DBE.

arrival at the endwall and the extrapolation of the maximum rate of the endwall OH* emission history to the baseline. Four equally spaced (30 cm), fast-response sidewall pressure transducers (PCB 113B26) are located along the end part of the driven section. The time interval between the instants of shock arrival at each pressure transducer location is obtained by three time counters (Fluke PM6690), with which the incident shock velocity at the endwall is determined by linear extrapolation. The OH* emission is detected by a photomultiplier (Hamamatsu, CR131) with a centered 306 ± 10 nm filter located at the endwall. All pressure and OH* signals are recorded by a digital acquisition instrument (Yokogawa DL750). The post-reflected shock temperatures were calculated by the chemical equilibrium program Gaseq.[22] All thermodynamic data of DBE, DME, DEE, argon, and oxygen were obtained from the Burcat database.[23]

The uncertainties of the ignition delay time were analyzed. In this study, the Fluke PM6690 time counters were used to measure the time intervals between the adjacent transducers. The counter uncertainty was estimated to be 1000 ns. The uncertainty of the measured distance is 0.02 mm in this study. The standard root-sum-squares (RSS) method was employed to calculate the uncertainty of the temperature behind the reflected shock wave. The temperature and its uncertainties are expressed as

$$T_5 = \frac{T_1[2(\gamma-1)M^2 + (3-\gamma)[(3\gamma-1)M^2 - 2(\gamma-1)]]}{(\gamma+1)^2M^2} = AM^2 + B + CM^{-2} \quad (1)$$

$$\delta V_s = \sqrt{\left(\frac{1}{\Delta t}\delta_{\Delta z}\right)^2 + \left(\frac{-\Delta z}{\Delta t^2}\delta_{\Delta t}\right)^2} \quad (2)$$

$$\delta T_5 = \frac{\partial T_5}{\partial M}\delta M = (2AM - 2CM^{-3})\frac{\delta V_s}{\sqrt{\gamma_1 R T_1}} \quad (3)$$

where T_1 is the initial temperature, γ is the gas-specific heat ratio, M is the incident-shock Mach number, R is the universal ideal gas constant (8314 J kmol^{-1} K^{-1}), V_s is the measured shock velocity, and z and t are the finite distance and time between pressure transducers, respectively. The distance interval of pressure transducers is 300 mm. For a given initial temperature (T_1 = 300 K) and gas-specific heat ratio (γ_1 = 1.67), the calculated temperature errors for T_5 = 1200 K (M = 2.17) and 1570 K (M = 2.55) are about 7 and 11 K, respectively. These temperature discrepancies lead to the experimental error on ignition delay time of less than 10%. The pressure rise before ignition is negligible for short ignition delay times, as discussed in our previous work.[24,25] Error bars were added to the measured data to reflect the uncertainty.

A recently developed kinetic model by Cai et al.[20] was employed to calculate the ignition delay times of DBE. This model has been validated against the ignition delay times at low temperatures and laminar flame speeds at atmosphere pressure. Simulations of ignition delay times were performed through the constant volume homogeneous reactor in CHEMKIN II package[26] assuming a zero-dimensional and constant volume adiabatic model. The simulated ignition delay time is defined as the time interval between the beginning of the reaction and the maximum rate of temperature rise (maximum dT/dt).

3. RESULTS AND DISCUSSION

In this section, ignition delay times of DBE at high temperatures were measured at different pressures, dilution ratios, and equivalences and comparisons to the predictions using a recently developed model were presented. The model yields good performance in the prediction of the ignition delay times. The ignition kinetics are then explored on the basis of the model. At last, a comparison of high-temperature ignition delay times of DBE to DME and DEE was given.

3.1. Ignition Delay Time Dependence. Figure 2 shows the comparison between the experimental results and model predictions for the DBE/O_2/Ar mixtures at an equivalence ratio of 1.0, a dilution ratio of 21, and pressures of 1.2, 2.0, and 4.0 bar. The ignition delay time is significantly decreased when the pressure is increased because of the increased absolute reactant concentration. The raw data for other mixtures (provided in the Supporting Information) show a similar dependence upon the pressure. This is consistent with the ignition behaviors of all alkane fuels under high-temperature conditions. Results show that model predictions give fairly good agreement to the experimental results under all conditions. Because of the low vapor pressure of DBE, the ignition delay times at higher pressures up to 10 bar were not measured in the present facility.

dx.doi.org/10.1021/ef500873e | Energy Fuels 2014, 28, 5489−5496

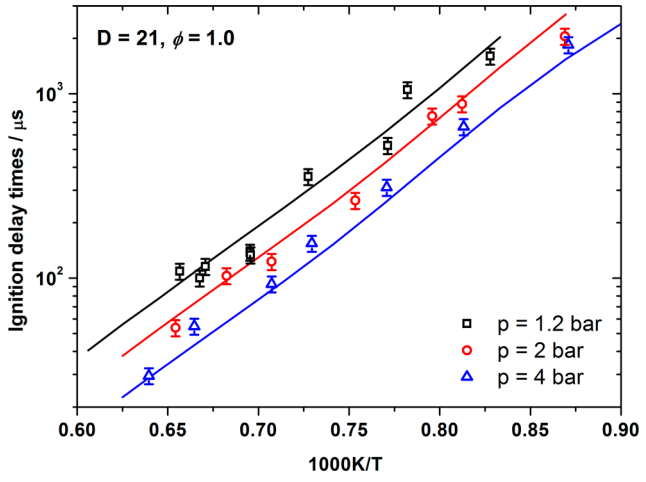

Figure 2. Effects of the pressure on ignition delay times of mixture 5, with D = 21 and ϕ = 1.0: (symbols) measurements and (solid lines) Cai's model.

Panels a and b of Figure 3 illustrate the effect of the dilution ratio on the ignition delay time at elevated pressures. Figure 3a gives the ignition delay times of mixtures 1, 3, and 5 (D = 21, 15.5, and 9.9, respectively) at an average pressure of 1.2 bar

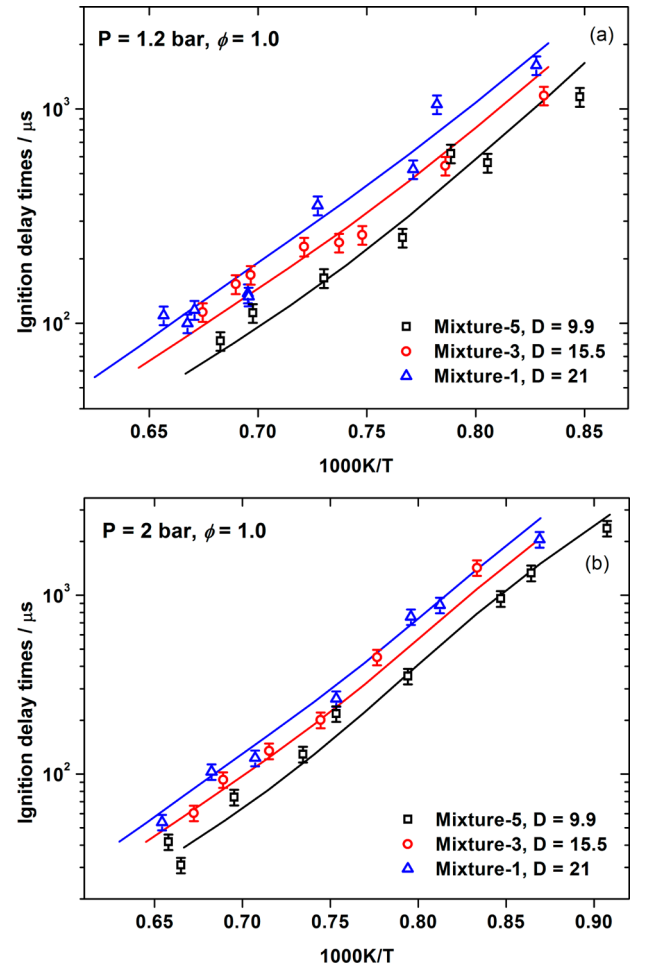

Figure 3. Effects of the dilution ratio on ignition delay times of DBE at different pressures: (symbols) measurements and (solid lines) Cai's model.

under stoichiometric conditions. Results show that the ignition delay time is increased with the increase of the dilution ratio (argon concentration). This is reasonable because, for a given equivalence ratio, an increase in the dilution ratio decreases the concentrations of both fuel and oxidizer, leading to a reduced overall reactivity.

Figure 3b gives the shock-tube data at a pressure of 2.0 bar. Similar trends were presented as that at a pressure of 1.2 bar. At high temperatures (1100−1570 K), lean mixtures are the slowest to be ignited and rich mixtures are the fastest. As shown in panels a and b of Figure 3, good agreement between experimental and numerical results is demonstrated.

Panels a and b of Figure 4 give the effect of the equivalence ratio on the ignition delay time. Figure 4a shows the data for

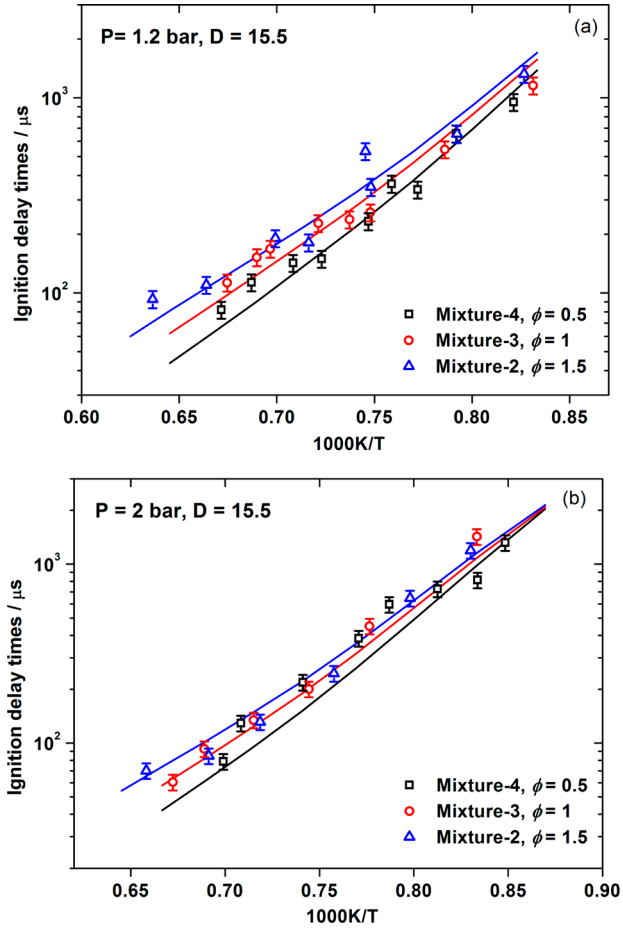

Figure 4. Effects of the equivalence ratio on ignition delay times for DBE at different pressures: (symbol) measurements and (solid lines) Cai's model.

mixtures 2, 3, and 4 (ϕ = 1.5, 1.0, and 0.5, respectively) at a fixed dilution ratio of 15.5 and a pressure of 1.2 bar. Similar to the observation from Healy et al.[27] in isobutane and Wei et al. in 2-methlyfuran,[28] a strong negative dependence of the ignition delay time upon the equivalence ratio at high temperatures ($1100 \leq T \leq 1570$ K) is demonstrated, indicating the high reactivity of the fuel-lean mixtures. This is because, in this temperature range, the dominant chain-branching reaction $H + O_2 \rightarrow O + OH$ is favored at higher oxygen concentrations and smaller equivalence ratios. As shown in Figure 4a, the dependence upon the equivalence ratio is well-captured by Cai's model and quantitative agreement between the model

dx.doi.org/10.1021/ef500873e | Energy Fuels 2014, 28, 5489−5496

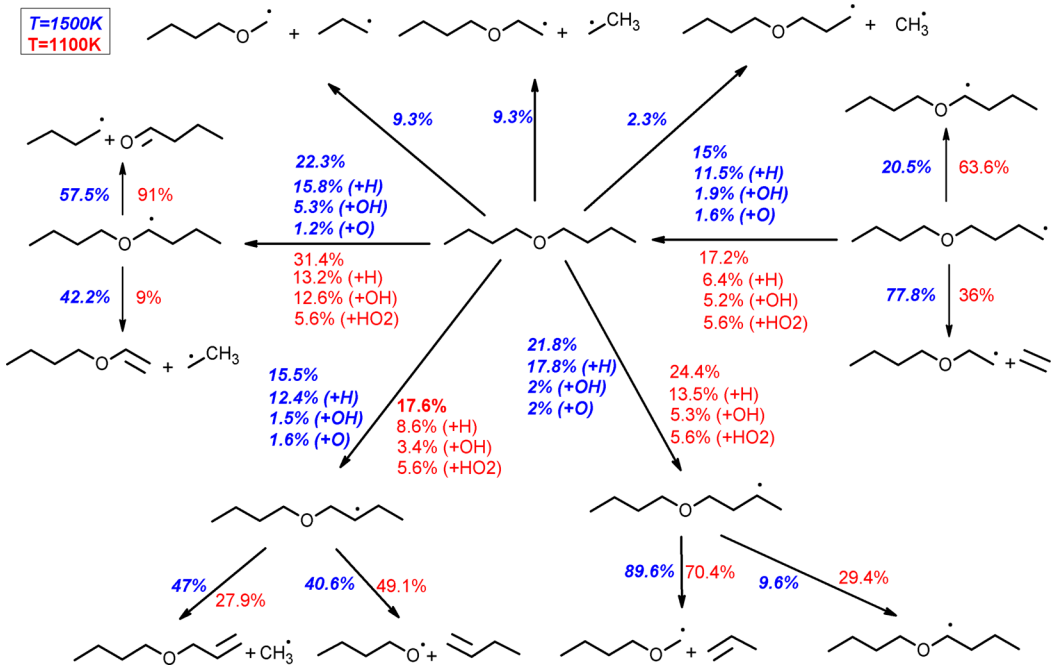

Figure 5. Reaction pathway diagram of mixture 3 oxidation in a shock tube at a pressure of 1.2 bar at 30% fuel consumption.

predicted and measured ignition delay times was observed. Furthermore, as the temperature is decreased, both measurements and model predictions show that the difference among the ignition delay times of the different equivalence ratio mixtures is decreased. Figure 4b shows the ignition delay time for different equivalence ratios at the pressure of 2 bar. A similar dependence of the ignition delay time upon the equivalence ratio, as that in Figure 4a, is presented. However, when the temperature decreases to about 1150 K, the difference among the ignition delay times of these three mixtures tends to decrease. It is speculated that, if the temperature was further decreased, the ignition delay time dependence upon the equivalence ratio is likely to be reversed. This behavior is consistent with the observations by Stranic et al.[29] for *n*-butanol and Wei et al.[28] for 2-methlyfuran. At relatively high pressures, the HO_2 chemistry becomes important and a rich mixture favors the sequences of fuel + HO_2 → R + H_2O_2, followed by H_2O_2 + M → OH + OH + M.

3.2. Kinetic Analysis. The reaction pathway flux of DBE ignition was performed at two initial temperatures (1100 and 1500 K), pressure p = 1.2 bar, equivalence ratio ϕ = 1.0, and dilution ratio D = 15.5, as shown in Figure 5. The instant of 30% fuel consumption is selected for the analysis.

At a temperature of 1100 K, the consumption of DBE is dominated by H-abstraction reactions. The H-abstraction reactions are dominated by H, OH, and HO_2 attack, and nearly no unimolecular decomposition reactions contribute to the fuel consumption at this temperature. At a temperature of 1500 K, although fuel destruction is still dominated by the H abstractions, the unimolecular decomposition of DBE has accounted for about 20.9% of the fuel consumption. This results from the high activation energy at high temperatures, leading to the increased importance of the unimolecular decomposition reactions. Additionally, this unimolecular decomposition by C_α−C_β and C_β−C_γ breaks contribute equally (9.3%), while the break of C_γ−C_δ only accounts for 2.3% of the fuel consumption, even though, in the model, the rate constants of all fuel C−C bond break reactions were estimated to be the same. For the H-abstraction reactions, the H abstraction from DBE by the HO_2 radical becomes more important at 1100 K compared to that at 1500 K, with the contribution up to 22.4%. At both temperatures, the H abstraction from the α-carbon site has the largest branching ratio, because of the smallest bond dissociation energy (BDE) of DBE at α carbon.

The reaction pathways of the four primary fuel radicals ($C_4H_9OC_4H_8$-a, $C_4H_9OC_4H_8$-b, $C_4H_9OC_4H_8$-c, and $C_4H_9OC_4H_8$-d) produced through H abstractions are all further degenerated through the β scission. However, there is a significant difference between the products of the β scission at the temperatures of 1100 and 1500 K. For instance, for the fuel radical $C_4H_9OC_4H_8$-a destruction at 1100 K, the primary products (91%) are butanal (C_3H_7CHO) and 1-butyl radical (C_4H_9), while at 1500 K, only 57.5% of its destruction goes through this channel and another 42.2% of the fuel radical goes to another channel, which produces *n*-butyl vinyl ether ($C_4H_9OC_2H_3$) and ethyl butanal (C_2H_5). The β scission of $C_4H_9OC_4H_8$-b and $C_4H_9OC_4H_8$-c radicals also goes through different channels at different temperatures. For the $C_4H_9OC_4H_8$-d radical, 63.6% isomerizes to form $C_4H_9OC_4H_8$-b and the remaining 36% goes through the β scission to form *n*-butyl vinyl ether ($C_4H_9OC_2H_3$) and ethylene (C_2H_4) at 1100 K, while at 1500 K, the isomerization channel is less significant (20%) and the β scission becomes more important to its destruction. This is consistent with the observation by Zhang et al.[30] that, for the *n*-butanol oxidation, the isomerization of the δ-fuel radical plays a significant role at relatively lower temperatures compared to the β-scission channel.

The sensitivity analysis under the same conditions as that of the reaction pathway analysis was conducted to identify the dominant reactions for the ignition delay time prediction. The normalized sensitivity coefficient is defined as

dx.doi.org/10.1021/ef500873e | *Energy Fuels* 2014, 28, 5489−5496

$$S = \frac{\tau(2.0k_i) - \tau(0.5k_i)}{1.5\tau(k_i)} \quad (4)$$

where τ is the ignition delay time and k_i is the reaction rate of the ith reaction in the mechanism. Negative S indicates a decrease in the ignition delay time and a promoted effect on the overall reactivity and vice versa.

Figure 6 presents the 15 most sensitive reactions for mixture 3 at a pressure of 1.2 bar and temperatures of 1100 and 1500 K.

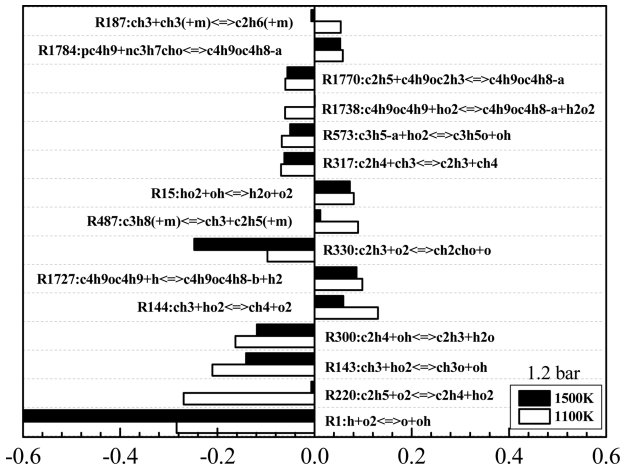

Figure 6. Normalized sensitivity of the ignition delay time for mixture 3.

It is found that the main chain-branching reaction R1 presents the largest negative sensitivity. The methyl radical reaction $CH_3 + HO_2 = CH_3O + OH$ is a chain-branching reaction and promotes the ignition, while $CH_3 + HO_2 = CH_4 + O_2$ is a chain-terminating reaction and inhibits the ignition. The ethane reaction R187, as two methyl radicals compose to an ethane, has negative sensitivity at high temperatures and positive sensitivity at low temperatures, which indicates that increasing the reaction rate can increase the activation energy. It is also observed that, besides the reactions of small radicals, which are expected to be important at this high temperature, some fuel-specific reactions are also important, such as the H-abstraction reactions (R1727) and the decomposition of α-fuel radicals (R1784 and R1770). The H-abstraction reaction by a hydrogen atom from the fuel strongly inhibits the reactivity because it consumes the H radicals and forms a stable hydrogen. In addition, reaction R1738 promotes the reactivity because it consumes a hydroperoxyl radical and produces a more active radical hydrogen peroxide (H_2O_2), which then dissociates to form two OH radicals. Reactions R1770 and R1784 involve the destruction of the fuel radical $C_4H_9OC_4H_8$-a. Through reaction R1770, n-butyl vinyl ether ($C_4H_9OC_2H_3$) and ethyl butanal (C_2H_5) were produced, which provide the reactants for a sequence of ignition promotion reactions, such as R220, R300, and R143, as shown in Figure 6. Reaction R1784, which produces 1-butyl radical (C_4H_9) radical, shows the positive coefficients and exhibits the negative influence on the reactivity. Reaction pathway analysis also reveals that, at the temperature of 1100 K, more α radicals decompose to 1-butyl radical and butanal, leading to the decreased reactivity and inhibited ignition.

3.3. Comparison to DME and DEE. Ethers, such as DME and DEE, are also important diesel fuel substitutes that have the same functional group as DBE, and to explore the effect of the length of the ether function group, comparisons of the high-temperature ignition delay times of DBE to DME and DEE are provided. Figure 7 shows the numerical and experimental

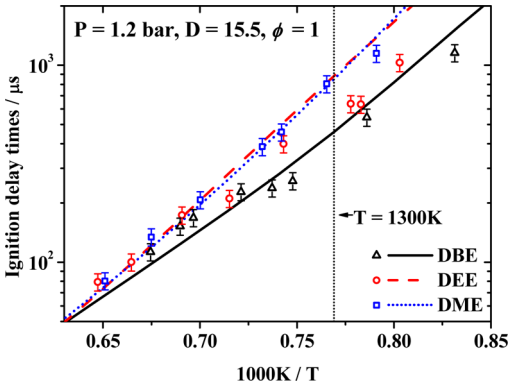

Figure 7. Measured and calculated ignition delay times of fuel/O_2/Ar mixtures at ϕ = 1.0, D = 15.5, and p = 1.0 bar.

ignition delay times for stoichiometric DME/O_2/Ar, DEE/O_2/Ar, and DBE/O_2/Ar mixtures at p = 1.2 bar and D = 15.5. The kinetic models proposed by Yasunaga et al.[16] and Metcalfe et al. (NUIG Aramco Mech 1.3)[31] were used to simulate the ignition delay time of DEE and DME, respectively. Results show that, at a temperature of about 1500 K, measurements show that three ethers have similar ignition delay times. As the temperature decreases, the difference among the three ethers becomes significant. DBE shows the shortest ignition delay times, while DME shows the longest ignition delay times, with the ignition delay times of DEE located between the two. Figure 7 also reveals that the length of the carbon chain of ethers has a big impact on the ignition delay times, especially at low temperatures. Ethers with the longer carbon chain length have shorter ignition delay times, and this is similar to the behavior of n-alcohols, in which long carbon length corresponds to short ignition delay times.[32] Moreover, the measured and calculated ignition delay times of DME and DBE present an excellent agreement, while the numerically predicted ignition delay times of DEE using Yasunaga's model[16] are significantly higher than the measurements. In the work by Yasunaga et al., we could also find that the model slightly overpredicted the ignition delays for the DEE/oxygen mixtures at equivalence ratios of 0.5 and 1. Thus, further experimental and theoretical studies on DEE should be conducted in the future, for the validation and optimization of the model.

To interpret the relative ignition delay times with different chain-length esters from the chemical kinetic point of view, Figures 8−11 present the sensitivity coefficients, the temperature evolution, and the reactant and radical profiles, respectively, for the DME/O_2/Ar, DEE/O_2/Ar, and DBE/O_2/Ar mixtures at ϕ = 1.0, p = 1.2 bar, D = 15.5, and T = 1300 K. For the DME/O_2/Ar mixture at this temperature, as shown in Figure 8, NUIG Aramco Mech 1.3 states that the DME dissociation reaction CH_3OCH_3 (+M) = CH_3 + CH_3O (+M) has even higher sensitivity coefficients than the main chain-branching reaction H + O_2 = OH + O. Additionally, the H-abstraction reaction of the molecular DME acts as the most ignition-inhibiting reaction. For the mixture of either DEE/O_2/Ar or DBE/O_2/Ar, the main chain-branching reaction H + O_2 = O + OH has the highest sensitivity coefficients among their

dx.doi.org/10.1021/ef500873e | Energy Fuels 2014, 28, 5489−5496

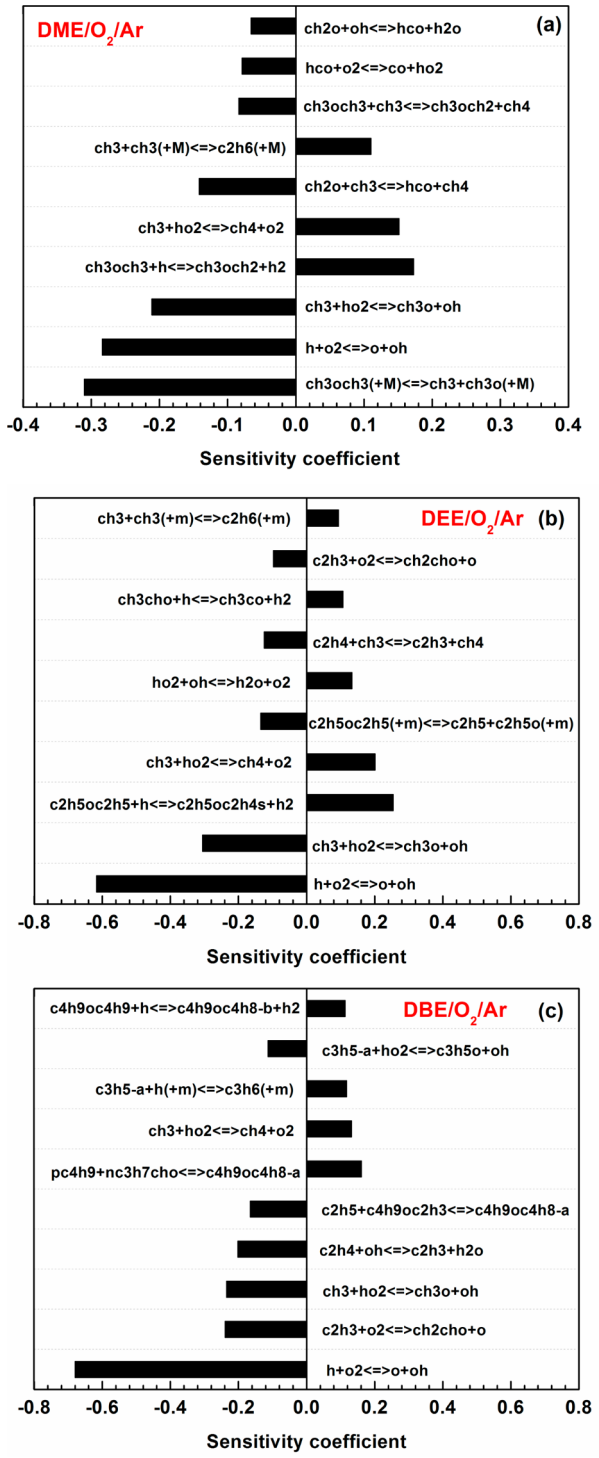

Figure 8. Ignition delay time sensitivity of fuel/O_2/Ar mixtures at ϕ = 1.0, D = 15.5, p = 1.2 bar, and T = 1300 K.

specific oxidation scheme. Furthermore, Figure 8b shows that the H-abstraction reaction $C_2H_5O(C_2H_5)$ + H = C_2H_5O-(C_2H_4) + H_2 is the most important ignition inhibiting reaction, and the fuel decomposition reaction of DEE has a noticeable negative sensitivity coefficient. Figure 8c shows that the α-fuel radical decomposition reactions of DBE are important in the prediction of the ignition delay time, as discussed in section 3.2. The H-abstraction reaction is also found to have a noticeable positive sensitivity coefficient, although not as significant as the H abstraction of DME and DEE in panels a and b of Figure 8.

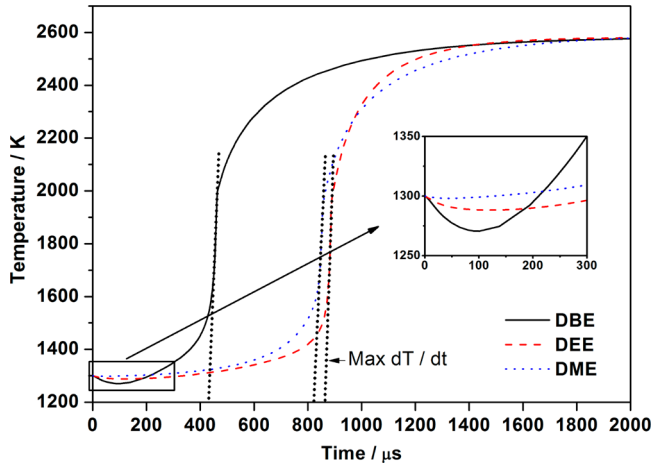

Figure 9. Computed temperature of fuel/O_2/Ar mixtures at ϕ = 1.0, D = 15.5, p = 1.2 bar, and T = 1300 K.

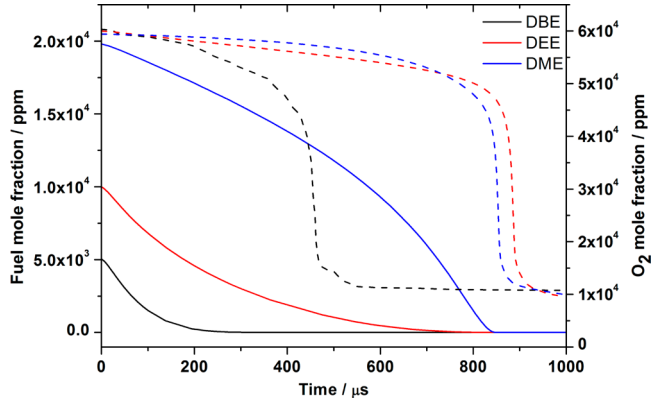

Figure 10. Mole fraction of fuel and O_2 for fuel/O_2/Ar mixtures at ϕ = 1.0, D = 15.5, p = 1.2 bar, and T = 1300 K: (solid lines) fuel and (dash lines) O_2.

Figure 9 plots the computed temperature profiles for the stoichiometric DME/O_2/Ar, DEE/O_2/Ar, and DBE/O_2/Ar mixtures at p = 1.2 bar, D = 15.5, and T = 1300 K. Initially, the temperature of DBE is decreased, and similar behaviors were observed for DME and DEE ignition, although not as significant as that for DBE. This is because the initial fuel decomposition is endothermic and produces radicals. When the radicals accumulate to a sufficient concentration, the exothermic reactions increase the system temperature. The temperature of DBE rises remarkably at around 400 ms, which is roughly the ignition delay times of DBE at 1300 K in Figure 7. The steep temperature rises for DEE and DME were observed at around 800 ms.

Figure 10 presents the fuel and oxygen mole fractions for the stoichiometric DME/O_2/Ar, DEE/O_2/Ar, and DBE/O_2/Ar mixtures at p = 1.2 bar, D = 15.5, and T = 1300 K. DME has the highest mole fraction, followed by DEE and DBE, while the oxygen concentrations for the three mixtures are almost equivalent. DBE was consumed significantly faster than DEE and DME. This reveals a stronger overall reactivity of DBE, although the absolute reactant concentration of DBE/O_2/Ar is smaller than those of DEE and DME. If we assume that the overall reaction rate to be w, $w \sim k(T)p^n$, where $k(T)$ is the reaction rate constant, which is proportional to $\exp(-E_a/RT)$, p is the partial pressure of the reactants, which represents the

dx.doi.org/10.1021/ef500873e | Energy Fuels 2014, 28, 5489−5496

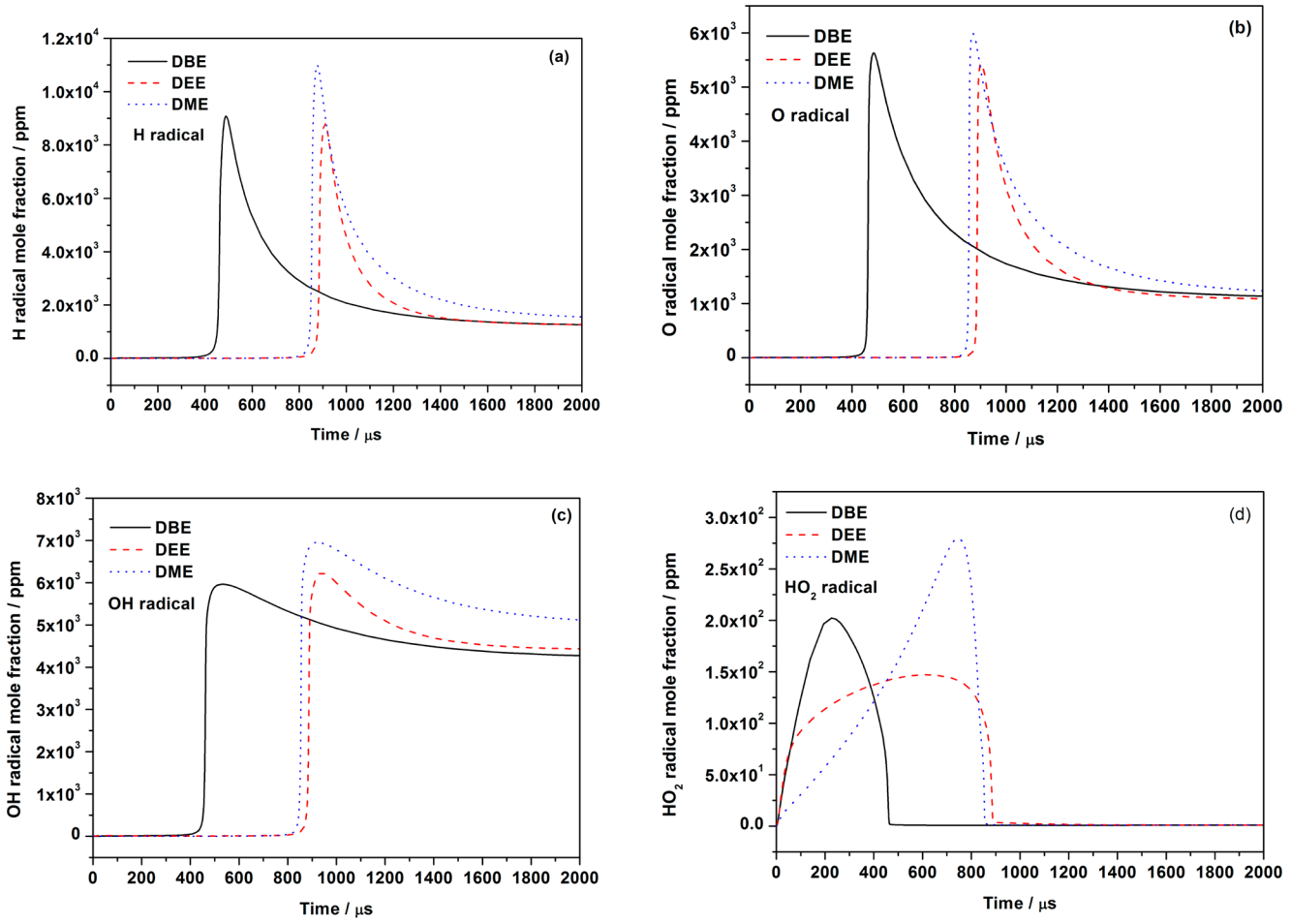

Figure 11. Mole fraction of free radicals of fuel/O_2/Ar mixtures at ϕ = 1.0, D = 15.5, p = 1.2 bar, and T = 1300 K.

absolute concentration factor, and n is the overall reaction order. As shown in Figure 10, the fuel concentration factor of DBE actually decreases the overall reaction rate. However, because the overall activation energy of DBE is significantly smaller than those of DEE and DME, as evidenced by the gentler slope of the quasi-linear relation of $\tau \sim 1/T$ in Figure 7, and, thus, the overall $k(T)$ of DBE is higher, as a consequence, the overall reactivity of DBE is higher than those of DEE and DME. Further evidence of the stronger reactivity of DBE is shown in panels a–d of Figure 11. At this high temperature, the fuel is primarily consumed through the H-abstraction reactions, as shown in Figure 5, and the main H-abstraction agent radicals, such as H, O, OH, and HO_2, for DBE are accumulated to the maximum value much earlier compared to DEE and DME.

4. CONCLUSION

Ignition delay times of DBE/O_2/Ar mixtures were measured behind reflected shock waves over equivalence ratios of 0.5–1.5, average pressures of 1.2–4.0 bar, temperatures of 1100–1570 K. An available kinetic mechanism for DBE[20] was employed to simulate the ignition delay times and yields good agreement with experimental data under all test conditions. The ignition delay time increases with the decrease of the pressure and the increase of the dilution ratio. A strong negative dependence of the ignition delay time upon the equivalence ratio at high temperatures was found, while the difference among the ignition delay times is decreased when the temperature is decreased. Sensitivity analysis for DBE reveals that, besides the reactions of small radicals, which are important at this high temperature, some fuel-specific reactions are also important, such as the H-abstraction reactions (R1727) and decomposition of α-fuel radicals (R1784 and R1770). Reaction pathway analysis confirms that the consumption of DBE is dominated by H-abstraction reactions at lower temperatures. With the increase of the temperature, the unimolecular decomposition reactions become more important. Comparisons of the high-temperature ignition delay times of DBE, DME, and DEE were made, and the result shows similar ignition delay times at high temperatures among the three ethers. The difference among the three ethers becomes significant at reduced temperatures. Yasunaga's chemical model of DEE[16] yields remarkable overprediction for DEE at low temperatures, and further experimental and theoretical studies on DEE are necessary for validation and optimization. Sensitivity coefficients, temperature evolution, and profiles of reactants and radicals for the three ethers were used to interpret the relative ignition delay times of different chain length esters from the chemical kinetic point of view. DBE shows a stronger overall reactivity than DME and DEE.

■ ASSOCIATED CONTENT

Supporting Information

All experimental data of ignition delay times of DBE, DME, and DEE. This material is available free of charge via the Internet at http://pubs.acs.org.

dx.doi.org/10.1021/ef500873e | Energy Fuels 2014, 28, 5489–5496

AUTHOR INFORMATION

Corresponding Authors

*Fax: +86-29-82668789. E-mail: chenglongtang@mail.xjtu.edu.cn.

*Fax: +86-29-82668789. E-mail: zhhuang@mail.xjtu.edu.cn.

Notes

The authors declare no competing financial interest.

ACKNOWLEDGMENTS

This work is supported by the National Natural Science Foundation of China (51206131, 51306144, and 51136005) and the National Basic Research Program (2013CB228406).

REFERENCES

(1) Yaripour, F.; Baghaei, F.; Schmidt, I.; Perregaard, J. Catalytic dehydration of methanol to dimethyl ether (DME) over solid-acid catalysts. *Catal. Commun.* **2005**, *6* (2), 147−152.

(2) Varisli, D.; Dogu, T.; Dogu, G. Ethylene and diethyl-ether production by dehydration reaction of ethanol over different heteropolyacid catalysts. *Chem. Eng. Sci.* **2007**, *62* (18), 5349−5352.

(3) Vishwanathan, V.; Jun, K.-W.; Kim, J.-W.; Roh, H.-S. Vapour phase dehydration of crude methanol to dimethyl ether over Na-modified H-ZSM-5 catalysts. *Appl. Catal., A* **2004**, *276* (1), 251−255.

(4) Rahmanian, A.; Ghaziaskar, H. Continuous dehydration of ethanol to diethyl ether over aluminum phosphate−hydroxyapatite catalyst under sub and supercritical condition. *J. Supercrit. Fluids* **2013**, *78*, 34−41.

(5) Melin, K.; Hurme, M. Evaluation of lignocellulosic biomass upgrading routes to fuels and chemicals. *Cellul. Chem. Technol.* **2010**, *44* (4), 117.

(6) Di, Y.; Huang, Z.; Zhang, N.; Zheng, B.; Wu, X.; Zhang, Z. Measurement of laminar burning velocities and Markstein lengths for diethyl ether−air mixtures at different initial pressure and temperature. *Energy Fuels* **2009**, *23* (5), 2490−2497.

(7) Yu, J.; Lee, J.; Bae, C. Dimethyl ether (DME) spray characteristics compared to diesel in a common-rail fuel injection system. *SAE Tech. Pap. Ser.* **2002**, DOI: 10.4271/2002-01-2898.

(8) Arcoumanis, C.; Bae, C.; Crookes, R.; Kinoshita, E. The potential of di-methyl ether (DME) as an alternative fuel for compression-ignition engines: A review. *Fuel* **2008**, *87* (7), 1014−1030.

(9) Cinar, C.; Can, Ö.; Sahin, F.; Yucesu, H. S. Effects of premixed diethyl ether (DEE) on combustion and exhaust emissions in a HCCI−DI diesel engine. *Appl. Therm. Eng.* **2010**, *30* (4), 360−365.

(10) Bailey, B.; Eberhardt, J.; Goguen, S.; Erwin, J. Diethyl ether (DEE) as a renewable diesel fuel. *Training* **1997**, *2014*, 6−11.

(11) Dagaut, P.; Boettner, J.-C.; Cathonnet, M. Chemical kinetic study of dimethylether oxidation in a jet stirred reactor from 1 to 10 ATM: Experiments and kinetic modeling. *Symp. (Int.) Combust., [Proc.]* **1996**, *26* (1), 627−632.

(12) Fischer, S.; Dryer, F.; Curran, H. The reaction kinetics of dimethyl ether. I: High-temperature pyrolysis and oxidation in flow reactors. *Int. J. Chem. Kinet.* **2000**, *32* (12), 713−740.

(13) Curran, H.; Fischer, S.; Dryer, F. The reaction kinetics of dimethyl ether. II: Low-temperature oxidation in flow reactors. *Int. J. Chem. Kinet.* **2000**, *32* (12), 741−759.

(14) Curran, H.; Pitz, W.; Westbrook, C.; Dagaut, P.; Boettner, J. C.; Cathonnet, M. A wide range modeling study of dimethyl ether oxidation. *Int. J. Chem. Kinet.* **1998**, *30* (3), 229−241.

(15) Zhao, Z.; Chaos, M.; Kazakov, A.; Dryer, F. L. Thermal decomposition reaction and a comprehensive kinetic model of dimethyl ether. *Int. J. Chem. Kinet.* **2008**, *40* (1), 1−18.

(16) Yasunaga, K.; Gillespie, F.; Simmie, J.; Curran, H.; Kuraguchi, Y.; Hoshikawa, H.; Yamane, M.; Hidaka, Y. A multiple shock tube and chemical kinetic modeling study of diethyl ether pyrolysis and oxidation. *J. Phys. Chem. A* **2010**, *114* (34), 9098−9109.

(17) Beeckmann, J.; Aye, M.; Gehmlich, R.; Peters, N. Experimental investigation of the spray characteristics of di-*n*-butyl ether (DNBE) as an oxygenated compound in diesel fuel. *Stroke* **2015**, 06−22.

(18) Nabi, M. N.; Ogawa, H.; Miyamoto, N. Approaches to extremely low emissions and efficient diesel combustion with oxygenated fuels. *Int. J. Engine Res.* **2000**, *1* (1), 71−85.

(19) Harry, C.; Arey, J.; Atkinson, R. Rate constants for the reactions of OH radicals and Cl atoms with di-*n*-propyl ether and di-*n*-butyl ether and their deuterated analogs. *Int. J. Chem. Kinet.* **1999**, *31* (6), 425−431.

(20) Cai, L.; Sudholt, A.; Lee, D. J.; Egolfopoulos, F. N.; Pitsch, H.; Westbrook, C. K.; Sarathy, S. M. Chemical kinetic study of a novel lignocellulosic biofuel: Di-*n*-butyl ether oxidation in a laminar flow reactor and flames. *Combust. Flame* **2014**, *161* (3), 798−809.

(21) Zhang, Y.; Huang, Z.; Wei, L.; Zhang, J.; Law, C. K. Experimental and modeling study on ignition delays of lean mixtures of methane, hydrogen, oxygen, and argon at elevated pressures. *Combust. Flame* **2012**, *159* (3), 918−931.

(22) Morley, C. *Gaseq, Version 0.76*; http://www.gaseq.co.uk.

(23) Goos, E.; Burcat, A.; Ruscic, B. http://garfield.chem.elte.hu/Burcat/THERM.DAT.

(24) Tang, C.; Man, X.; Wei, L.; Pan, L.; Huang, Z. Further study on the ignition delay times of propane−hydrogen−oxygen−argon mixtures: Effect of equivalence ratio. *Combust. Flame* **2013**, *160* (11), 2283−2290.

(25) Tang, C.; Wei, L.; Man, X.; Zhang, J.; Huang, Z.; Law, C. K. High temperature ignition delay times of C5 primary alcohols. *Combust. Flame* **2013**, *160* (3), 520−529.

(26) Kee, R. J.; Rupley, F. M.; Miller, J. A. *Chemkin-II: A Fortran Chemical Kinetics Package for the Analysis of Gas-Phase Chemical Kinetics*; Sandia National Laboratories: Livermore, CA, 1989; Report SAND89-8009.

(27) Healy, D.; Donato, N.; Aul, C.; Petersen, E.; Zinner, C.; Bourque, G.; Curran, H. Isobutane ignition delay time measurements at high pressure and detailed chemical kinetic simulations. *Combust. Flame* **2010**, *157* (8), 1540−1551.

(28) Wei, L.; Tang, C.; Man, X.; Huang, Z. Shock-tube experiments and kinetic modeling of 2-methylfuran ignition at elevated pressure. *Energy Fuels* **2013**, *27* (12), 7809−7816.

(29) Stranic, I.; Chase, D. P.; Harmon, J. T.; Yang, S.; Davidson, D. F.; Hanson, R. K. Shock tube measurements of ignition delay times for the butanol isomers. *Combust. Flame* **2012**, *159* (2), 516−527.

(30) Zhang, J.; Wei, L.; Man, X.; Jiang, X.; Zhang, Y.; Hu, E.; Huang, Z. Experimental and modeling study of *n*-butanol oxidation at high temperature. *Energy Fuels* **2012**, *26* (6), 3368−3380.

(31) Metcalfe, W. K.; Burke, S. M.; Ahmed, S. S.; Curran, H. J. A hierarchical and comparative kinetic modeling study of C_1−C_2 hydrocarbon and oxygenated fuels. *Int. J. Chem. Kinet.* **2013**, *45* (10), 638−675.

(32) Zhang, J.; Niu, S.; Zhang, Y.; Tang, C.; Jiang, X.; Hu, E.; Huang, Z. Experimental and modeling study of the auto-ignition of *n*-heptane/*n*-butanol mixtures. *Combust. Flame* **2013**, *160* (1), 31−39.